Journal of Power Sources 268 (2014) 153–162

Contents lists available at ScienceDirect

Journal of Power Sources

journal homepage: www.elsevier.com/locate/jpowsour

Review

The formation and stability of the solid electrolyte interface on the graphite anode

Victor A. Agubra*, Jeffrey W. Fergus

Materials Research and Education Center, Auburn University, 275 Wilmore Laboratories, Auburn, AL 36849, USA

HIGHLIGHTS

- The stability of the SEI layer remains a challenge in batteries performance.
- Carbonaceous anode electrode by far forms the most stable SEI layer.
- The development of solvent additives and carbon surface modifications is on-going.
- More research efforts in the area of improving SEI stability are still needed.

ARTICLE INFO

Article history:
Received 26 April 2014
Received in revised form
26 May 2014
Accepted 4 June 2014
Available online 24 June 2014

Keywords:
Lithium ion batteries
Solid electrolyte interphase
Graphite anode
Electrolyte decomposition

ABSTRACT

The solid electrolyte interface (SEI) layer plays a critical role in the cycle life of Li-ion batteries. The potential difference across the SEI during charging results in the potential for Li^+ intercalation at the graphite-SEI interface to be lower than the potential at the SEI-electrolyte interface, which can prevent electrolyte reduction and decomposition. The stability of the SEI layer at certain critical battery operating conditions remains a challenge in the performance of lithium ion batteries. Electrolyte additives and surface modification of the anode electrode have been shown to improve the formation of an effective SEI layer. However, there is still a need for improving the robustness of the SEI to withstand extreme battery operating conditions. In this paper, the formation and stability of the SEI layer for lithium ion batteries is reviewed. This review includes discussion of the formation, growth and stability of the SEI on graphite anode materials.

1. Introduction

The reaction of the anode with the electrolyte solution in the formation stage results in the formation of various surface species on the electrode surface. This surface film is commonly referred to as solid electrolyte interphase (SEI). The SEI layer is a Li^+ conductor but an insulator to electron flow and limits further electrolyte decomposition to improve the cycle life performance of the Li-ion batteries. This thus makes the SEI film an important part of the electrochemical process in the lithium ion batteries. The most commonly used anode materials for lithium ion batteries are the carbon-based compounds and lithium alloys, which has mostly been reported to form good SEI film [1–8].

Generally, the passive state of the SEI layer occurs during charging when the electrolyte decomposes into various species that lead to the formation of a variety of layers on the electrode surface [9]. Electrolyte salts, such as $LiPF_6$, $LiAsF_6$, LiBOB, $LiClO_4$ or $LiBF_4$, in a mixture of carbonate solvents are widely used electrolyte solutions [6–10]. These salts and solvents are reduced at potential that is higher than the intercalation potential of lithium ions, resulting in the precipitation of various species on the surface of the graphite anode to form the SEI layer [11–14].

When lithium ion batteries are subjected to certain extreme battery operation conditions, such as prolonged electrochemical cycles, high temperature (>60 °C) and high charge rate, the formed SEI either grows in thickness or becomes non-protective, which leads to performance degradation through several aging mechanisms [12,15,17]. The carbonate solvents, with the exception of propylene carbonate, have been widely reported to form stable and robust SEI layers with the common electrolyte salt, $LiPF_6$ [18–21]. However, the propylene carbonate (PC) performs well as a solvent at low temperatures but is rarely used alone as it exfoliates the graphite electrode, allows solvent co-intercalation, and inhibits Li^+ intercalation. The electrolyte composition and its properties are therefore key to the formation of an effective SEI layer.

* Corresponding author. Tel.: +1 3348443353; fax: +1 3348443400.
E-mail address: vaa0002@auburn.edu (V.A. Agubra).

http://dx.doi.org/10.1016/j.jpowsour.2014.06.024
0378-7753/

In addition to the electrolyte composition, the electrode materials also play a critical role in the formation of an effective SEI layer. The SEI layer formed on carbon-based anodes in common electrolytes salts and carbonate solvents generally have better microstructures and are more effective [22–25] as compared to other anode materials [26–29]. This paper will focus is on the formation and stability of the SEI layer on the commonly used carbon based anode electrode and the SEI layer affects the performance of the lithium ion batteries.

2. Solvent reduction

The reduction of carbonate solvents follows either one-electron reduction process. As in the case of ethyl methyl carbonate (EMC), which is reduced by a one-electron process in Eq. (1)

$$CH_3CH_2O(C{=}O)OCH_3 + e^- \rightarrow CH_3CH_2O\left(C^{\bullet} - O^-\right)OCH_3 \quad (1)$$

to produce an intermediary; $CH_3CH_2O(C^{\bullet} - O^-)OCH_3$ which then reacts with Li^+ to produce the species CH_3CH_2OLi according to Eq. (2).

$$CH_3CH_2O\left(C^{\bullet} - O^-\right)OCH_3 + e^- + 2Li^+ \rightarrow LiO(C{=}O)CH_3 + CH_3CH_2OLi \quad (2)$$

Alternatively, a two-electron reduction process can occur, as in the case of dimethyl carbonate (DMC), (Eq. (3))

$$CH_3OCO_2CH_3 + 2e^- + 2Li^+ \rightarrow Li_2CO_3\downarrow + C_2H_{6(g)}\uparrow \quad (3)$$

where the reduction process involves the solvent molecule, a transfer of two-electrons, and Li^+ to produce a lithium carbonate species and a gas [14,22,31]. The ensuing discussion will however focus on the reduction of ethylene carbonate (EC) and propylene carbonate (PC) solvents with $LiPF_6$ as the salt, which are commonly used electrolytes.

2.1. Reduction of ethylene carbonate (EC)

In a mixture with other carbonate solvents, ethylene carbonate (EC) is preferably reduced due to its high polarity and dielectric constant [30]. Like the dimethyl carbonate (DMC) and diethyl carbonate (DEC) solvents, the reduction of EC also involves a two-electron [32] transfer to 1 mol EC molecules and reaction with Li^+ to produce Li_2CO_3 and C_2H_4 gas (Eq. (4))

$$(CH_2O)_2CO + 2e^- + 2Li^+ \rightarrow Li_2CO_3\downarrow + C_2H_{4(g)}\uparrow \quad (4)$$

or a two-electron transfer to 2 mol of EC and Li^+ to form a lithium alkyl carbonate specie, which is deposited on the graphite particles and CH_2 gas that remain in the solution with the electrolyte (Eq. (5)).

$$EC + 2e^- + 2Li^+ \rightarrow (CH_2OCO_2Li)_2\downarrow + CH_2{=}CH_{2(g)}\uparrow \quad (5)$$

The species $(CH_2OCO_2Li)_2$ on the graphite particles surface, can readily react with traces of H_2O in the solution to produce Li_2CO_3, $(CH_2OH)_2$ and CO_2 gas (Eq. (6)) [31,32]. The reaction with H_2O could therefore compound the amount of gases produced in the battery pack leading to cell venting. It is therefore imperative to keep the H_2O content in the electrolyte to minimal levels (<1000 pmm).

$$(CH_2OCO_2Li)_2 + H_2O \rightarrow Li_2CO_3\downarrow + (CH_2OH)_2\downarrow + CO_{2(g)}\uparrow \quad (6)$$

The EC solvent reduction, however, depends on the applied cell potential which ranges from 4.6 to 4.9 V vs. Li/Li^+ [33] to overcome the decomposition reaction barrier [30]. The EC molecules which is preferably solvated in a mixture of other carbonate solvents due to its high polarity, is a target for electrophilic and nucleophilic reactions [34,35]. In a presence of anionic species such as PF_6^-, ClO_4^-, BOB^-, F_2OB^-, AsF_6^-, and $CF_3SO_3^-$ from the corresponding electrolyte salts, $LiPF_6$, $LiClO_4$, LiBOB, LiF_2OB, $LiAsF_6$ and $LiCF_3SO_3$ respectively, trigger the ring opening and bond breaking of ethylene carbonate molecules are to form various species on the surface of the electrode. In particular, the decomposition species of POF_3 from $LiPF_6$ reduction, reacts with H_2O to form POF_3, (Eq. (7)):

$$PF_5 + H_2O \rightarrow 2HF + POF_3 \quad (7)$$

which reacts with EC to produce an intermediary CH_2FCH_2O-$COOPF_2O$ species by Eq. (8)

$$POF_3 + EC \rightarrow CH_2FCH_2OCOOPF_2O \quad (8)$$

The intermediary then further dissociates to form CH_2FCHO-$COOPF_2O$ and CO_2 according to Eq. (9).

$$CH_2FCH_2OCOOPF_2O \rightarrow CH_2FCH_2OPF_2O + CO_{2(g)}\uparrow \quad (9)$$

Another possible reaction involves the anion PF_6^- and the species POF_3, which can simultaneously attack the EC molecule to form the anion $CH_2FCH_2OCOOPF_3O^-$ and a Lewis acid according to Eq. (10),

$$POF_3 + EC + PF_6^- \rightarrow CH_2FCH_2OCOOPF_3O^- + PF_5 \quad (10)$$

which can dissociate further to form an additional anion in solution (Eq. (11))

$$CH_2FCH_2OCOOPF_3O^- + PF_5 \rightarrow CH_2FCHOCOOPF_2O + PF_6^- \quad (11)$$

to perpetuate the decomposition reaction [34]. This initiated autocatalytic process can be suppressed by adding a Lewis base complex to the PF_5 to form a stable acid-base [36].

Furthermore, the $LiPF_6$ salt, which is thermodynamically unstable [37], can react with Li_2CO_3 from EC reduction to produce LiF, POF_3 and CO_2 (Eq. (12)).

$$LiPF_6 + Li_2CO_3 \rightarrow 3LiF + POF_3 + CO_{2(g)}\uparrow \quad (12)$$

Alternatively, the $LiPF_6$ reduction species PF_5, readily reacts with Li_2CO_3 (Eq. (13)):

$$PF_5 + Li_2CO_3 \rightarrow 2LiF + POF_3 + CO_{2(g)}\uparrow \quad (13)$$

On the other hand, the HF species reacts with the Li_2CO_3, to produce CO_2 and H_2O (Eq. (14))

$$Li_2CO_3 + 2HF \rightarrow 2LiF + CO_2 + H_2O \quad (14)$$

Trace impurities of H_2O and CO_2 in solution are reported [38] to react with Li^+ to form Li_2CO_3, LiOH and Li_2O that form part of the SEI layer. The LiF species from these reactions with Li_2CO_3, however, are deposited on the electrode and form an insoluble, non-uniform and electronically insulating layer on the graphite particle surfaces (Fig. 1a) [39–41].These undesirable reactions reinforces the goal of keeping the H_2O levels in the electrolyte to the barest minimum.

These reaction products (LiF, Li_2CO_3, LiOH and Li_2O) on the electrode surface may crack (Fig. 1b) due to the differences in the coefficients of thermal expansion between the deposit layer and the graphite particles [33,42]. This phenomenon could allow further reaction at these newly created crevices on the electrode surface.

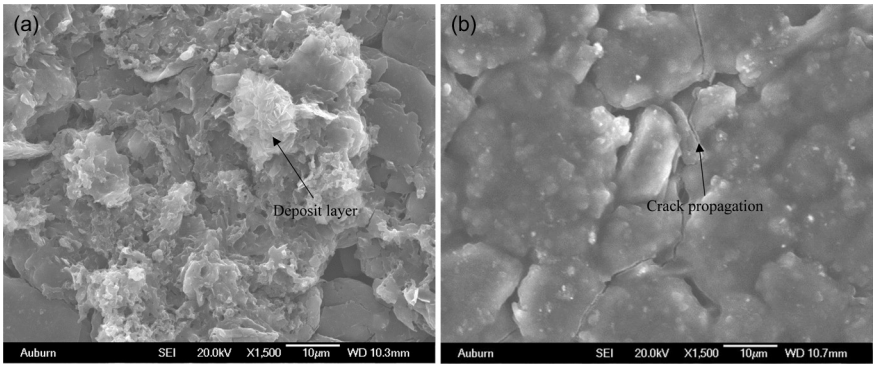

Fig. 1. (A) surface layer deposited on the graphite particles, (B) deposit layer showing cracks [6].

2.2. Propylene carbonate (PC)

In spite of PC decomposing and reacting with Li^+ to form a poor SEI layer and allowing solvent co-intercalation and exfoliation of the graphite electrode, it remains a good candidate for low temperature (<−10 °C) performance in lithium ion batteries. The common approach has often been to produce an effective surface film with PC by using electrolyte additives with a higher negative reduction potential compared to the PC. Thus such an additive reduction precedes that of the PC and reacts with Li^+ to form a protective layer on the carbon particles surface that prevents carbon exfoliation and solvent co-intercalation. The reaction of the electrode material with PC involves a one-electron transfer followed by radical termination. At potentials close to the anode electrode potential, PC easily decomposes to form superoxide ions through a nucleophilic attack on the carbon particles in the presence of oxygen. The O_2 superoxide radical then decomposes PC through this nucleophilic attack to form $(PC)_2LiOC(O)OCH(CH_3)CH_2OLi(PC)$ on the graphite electrode as a continuous process [43,44]. The reduction allows solvent co-intercalation [2]. In addition, the reduction of PC molecules also occurs on the edges of the graphite planes and causes exfoliation of the graphite [42]. The PC molecules therefore solvates Li^+ resulting in solvent co-intercalation of PC molecules with Li ions into graphite structure [43,44].

The PC reduction, which generally also involves a two-electron transfer from the electrode to the PC molecules and in the presence of Li^+ forms surface polymerized carbonate species, such as Li_2CO_3, $CH_3CH(OCO_2Li)CH_2OCO_2Li$ and propylene gas [2,45] (Eq. (15)).

$$PC + 2e^- + 2Li^+ \rightarrow CH_3CH(OCO_2Li)CH_2OCO_2Li + Li_2CO_3\downarrow + C_3H_{6(g)}\uparrow \quad (15)$$

The reduced products contain loose alkyl tails in the form of methyl groups, which prevents the formation of a compact SEI layer [46] on the graphite surface.

Some failures of the anode electrode in a PC solvent involve exfoliation of the carbon particles and the creation of crevices on the electrode. These fractures electronically disconnect the graphite particles from the current collector [16,20,43,47] rendering these particles electrochemically inactive. As mentioned earlier, one of the ways to improve PC performance is by adding some electrolyte additives. The vinylene carbonate (VC) electrolyte additive has been used extensively as an additive to PC solvents to produce a stable and robust SEI layer [6,12,34,36]. A Section 7.1 discusses the mechanism of the VC as an electrolyte additive in forming a stable SEI layer with some carbonate solvents especially PC.

Other methods, including heat treatment of the graphite, coating with a thin copper layer, and tris(2,2,2-trifluroethyl) phosphite, have been successful in preventing PC decomposition and exfoliation of graphite [48–50]. The heat treated graphite provides a high crystallinity surface that creates less energetic points for passivation reaction [49], while the copper coating and tris(2,2,2-trifluroethyl) phosphite prevents direct electrolyte contact with active carbon surface. Also, varying the ratio of PC/DEC solvent in $LiPF_6$ has been reported to suppress the decomposition of PC [51]. The suitable ratio creates no free molecules of PC and all molecules are solvated to lithium ions as $Li(PC)_2^+$.

3. Decomposition of $LiPF_6$ salt

The $LiPF_6$ salt is the most common electrolyte salt used in lithium ion batteries. The decomposition of $LiPF_6$ follows a two-step process in which the decomposition is related to the release of free acid followed by decomposition of the salt [52]. The initial reaction for the salt decomposition is electron transfer from the electrode to the salt molecule [53,54] to produce a toxic alkylfluorophosphate (A in Fig. 2). The alkylfluorophosphate reaction is initiated through autocatalytic from aprotic impurities of water or alcohol [36,55,57] in the electrolyte which accelerates the decomposition of $LiPF_6$ (B in Fig. 2).

The salt dissociates into LiF (C in Fig. 2), and the Lewis acid PF_5 (Eq. (16));

$$LiPF_6 \leftrightarrow LiF + PF_5 \quad (16)$$

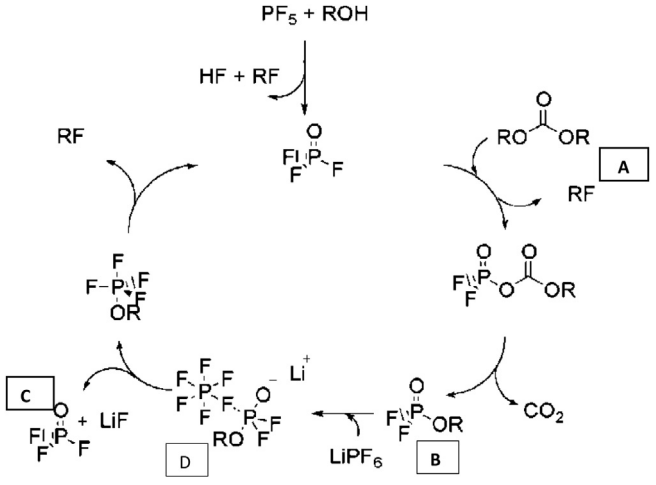

Fig. 2. Schematic of autocatalytic reaction mechanism for the LiPF6 [55] (Reproduced by permission The Electrochemical Society).

Table 1
Chemical reduction species for PC-based electrolytes and commonly used carbonate solvents.

Solvents		Salts	Li_2CO_3	$ROCO_2Li$	$(CH_2OCO_2Li)_2$	LiF	Others species
PC		LiPF $LiPF_6$	[12]			[12]	
		$LiAsF_6$	[15]	[15]			$CH_3CH_2CO_3Li$
		$LiClO_4$	FTIR [16,46,47,102,129]	[47,98,101,103]		[16]	$CH_3CH_2CO_3Li$, LiOH, Li_2O [16]
		$LiBF_4$	FTIR [1,8,45,47,94] [79,102,109]	[1,8,44,46,92,101] [103,108]			$LiOCO_2R$
PC	EC/DMC/DEC	$LiClO_4$	[79]	[79]	[79]		Li_2O $LiOCO_2R$
		$LiPF_6$	[1,8]	[8]	[8]		CH_3OCO_2Li, PEO, ROLi [8] Li_2O
	DMC/EC	LiPF6	FTIR [18,43]	[18,43]	[18]		Li_2O, LiOH ROLi
		$LiAsF_6$	XPS [58,76]	[76]	[58,76]	[58,76]	PEO [76]
	EC/DEC	$LiPF_6$	FTIR [3,45]	[3,45]	[3,45]		$CH_3CH_2CO_3Li$
		$LiAsF_6$	XPS [94]		[94]	[94]	
		$LiClO_4$	XPS [99]	[99]	[99]		LiOH [99]
		$LiBF_4$	FTIR [8,45,47,101,102,114]	[8,45,47,101,102,114]	[8,45,47]		

or a Li^+ and the anion PF_6^- as shown in Eq. (17).

$$LiPF_6 \leftrightarrow Li^+ + PF_6^- \quad (17)$$

The dissociated Lewis acid PF_5 can react with H_2O (Eq.(18)–(20)), existing as an impurity in solution or the alcohol to form POF_3, or PF_4OH and specie HF [32,42,52]

$$PF_5 + H_2O \rightarrow 2HF + POF_3 \quad (18)$$

$$PF_5 + H_2O \rightarrow PF_4OH + HF \quad (19)$$

The species PF_4OH can further dissociates to produce POF_3 and HF that remain in solution [55,57];

$$PF_4OH \rightarrow POF_3 + HF \quad (20)$$

The Lewis acid PF_5 can also react with dialkylcarbonate to form a variety of decomposition products; ethers (R_2O), alkylfluorides, and phosphorus oxyfluoride (OPF_3) [52,58–60]. The generated POF_3 reacts with the solvent DEC to produce $OPF_2OC_2H_5$ along with CO_2 and C_2H_5F. The generated ethylfluorophosphate in solution interacts with the anion PF_6^- and forms the complex labeled as D in Fig. 2. However, the stability of PF_5 in solution depends on the solvent, it is stable in polar sterically compact solvents, such as EC, while in less polar and bulky solvents such as DMC and DEC [58], the PF_5 species is often unstable.

The decomposition of $LiPF_6$ is further promoted by solvents with large dielectric constants and high viscosity [60,61], such as EC. Such high dielectric constant solvents increase the ionization of the salt and accelerates its reduction reaction and its subsequent reaction with water to form the LiOH species. When the salt anion and solvent are reduced simultaneously, their reduction reaction interferes to produce a less passive SEI film that is less protective [62]. This will cause the salt and solvent compositional change that eventually reduce the ionic conductivity of the electrolyte [64] and thus degrades its transport properties via conducting species depletion [65]. This however, depends on the electrode potential and the electrolyte composition [63]. This phenomena is usually corrected through proper electrode materials and electrolyte selection and electrode design, therefore does not often arise in most lithium ion batteries chemistries.

Some of the methods employed to minimize the thermal instability of the salt $LiPF_6$, include inhibiting the transesterification of dialkylcarbonate [57,60] and lowering the concentrations of protic impurities of H_2O and EtOH in the carbonate solvents [55,65–67]. The addition of inorganic compounds, such as tris (2,2,2-trifluroethyl) phosphite (TTFP) and low concentration of Lewis bases; pyridine, hexamethoxycyclotriphosphazene and hexamethylphosphoramide to the salt has also been used to improved thermal stability. The inorganic compounds inhibit the reactivity of the Lewis acid PF_5, which is the main cause of the instability of $LiPF_6$, to effectively improve the stability of $LiPF_6$ salt [65,68,69].

4. Surface film chemical products

The electrolyte salts in the presence of carbonate solvents form various reduction products on the surface of the electrode that constitute the SEI layer. The most commonly produced chemical

Table 2
Chemical reduction species for EC-based electrolytes and commonly used carbonate solvents.

Solvents		Salts	Li_2CO_3	$ROCO_2Li$	$(CH_2OCO_2Li)_2$	LiF	Others species
EC	EMC	$LiAsF_6$	FTIR [6,13]	[6,13]			CH_3OH, LiOH [13]
		$LiPF_6$	FTIR [18,23,70]	[18,70,104]	[18]		$LiHCO_3$ [18] PEO[CH_3OCO_2Li [71] LiOH, $LiOC_2O_4$, Li_2O [18]
	DEC	$LiClO_4$	[4,16,61,70,77,78,92,97,111]	[4,5,61,71,77,94,97]	[97]	XPS [16,97]	ROLi [97] LiOH, Li_2O [16]
		$LiAsF_6$	[37,61,100]	[61,101]	[39]	XPS [61,101]	Li_2O, LiOH [101]
		$LiPF_6$	[5,22,24,46,56,62,84,101]	[5,22–24,39,56,62,84,101]	FTIR [5,24,27,49,56,71,118]	XPS [5,24,55,83]	CH_3CH_2OLi [22,39] ROCOOR [5] $C_2H_5OCO_2Li$, Li_2O [84]
	DMC	$LiBF_4$	FTIR [13,17,32,76,94]	[13,17,32,77,94]	[13,32,77,94]		PEO, ROLi, LiOH [13,32,94]
		$LiClO_4$	XPS [26,89]	[26,89]	[26,89]	[19,89]	LiOH [19]
		$LiAsF_6$	[32,39,107]	[32,107]	[32,39]	[32]	ROLi, LiOH [32]
		$LiPF_6$	[13,20,26,32,59,80,94]	[13,32,59,80,94,110]	[13,26,94,110]	[11,13,24,32,75,93]	LiOH, CH_3OCO_2Li, PEO [13,26,80]
	DEC DMC	$LiAsF_6$	XPS [40,100]	[40,100]	[40,100]	[40,100]	$C_2H_5OCOOLi$ [100]
		$LiPF_6$	[7,17,31,75,83]	[17,31]	[3,31,75,83]	[31]	OPF_2OR, $C_2H_5OCOOLi$ [74] LiOH PEO [7,17]
	EMC/DMC	$LiPF_6$	FTIR [52,67,73]		[52,67,75]		LiOH $C_2H_5OCOOLi$,
	EMC	$LiPF_6$	XPS [108]	[108]	[108]		LiOH, Li_2O

species from carbonate solvents and most electrolyte salts are $ROCO_2Li$ and Li_2CO_3, and $(CH_2OCO_2Li)_2$ as shown in Tables 1 and 2. PC solvent alone reacting with the electrolyte salt does not produce the species $(CH_2OCO_2Li)_2$, which is formed as a result of the two-electron transfer to 2 mol of EC and Li^+ (Eq. (7)). The species LiF is also common but not detected in some studies presented in Tables 1 and 2. Analytical tools such as the Fourier transformed infrared spectroscopy (FTIR), X-ray photoelectron spectroscopy (XPS) and Raman spectroscopy are often used to identify these surface compounds. In FTIR, the chemical compounds identification are mostly associated with the asymmetric and symmetric stretching vibration of the C═O, C–O, C–H, C–O–C, and C–F bonds [5,19,45] in the IR spectrum. However, the absorbance of chemical species such as LiF and Li_2O occur at wavenumbers less than 180 cm^{-1}, which is lower that the frequency range of the FTIR. Therefore surface sensitive tools like XPS are often better tools to detect such species. Therefore, the reported presence or absence of these chemical species from the various studies largely depends on the analytical tool used. The salt impurity LiF in solution forms a resistive layer on the electrode [3,16,21,32,42,69–72] due to an increase in solution acidity at the end of charge reaction [31].

Batteries with PC solvent alone and salts as the electrolyte are rare, since there would not be lithium intercalation into the graphite crystal structure. Most of the cells presented in Table 1 use PC as a base solvent to carried out to electrode kinetics studies to in the view of designing a better PC based solvent with other carbonate electrolytes for low temperature operation [12,15,47]. A quaternary composition of PC and other carbonate solvents without any additive is reported to form an unstable SEI layer consisting of a variety of chemicals species [8], due to creation of no free molecules of PC as all molecules would be solvated. Most others include an electrolyte additive such as VC, to promote the formation of an effective SEI layer [3,43].

Ethylene carbonate is by far the most commonly used base solvent. In the solvent mixtures of EC/DEC, Li_2O is commonly produced, while in EC/DMC LiOH is produced, which is mostly associated with Li reacting with H_2O in the solvent. The solvent DMC is easily hydrolyzed in water to produce methanol and CO_2. Conversely, DEC is insoluble in water. The choice of a binary, ternary or quaternary solvent composition depends on the power and energy densities characteristic of the desired battery chemistry [17,37,61,67]. Some electrolyte formulations are developed to meet certain battery performance criteria such as: conductivity (eg. $LiPF_6$/EC:DMC:DEC:EMC), temperature range (high temperature: LiPF6/EC: EMC and low temperature: LiBOB/EC/DMC and LiPF6/EMC/VC), and voltage range stability [70]. This choice of electrolyte can significantly impact on the safety, thermal stability, and abuse tolerance of the cell.

In addition to the deposition of reduction species on the electrode surface, gaseous products such as CO_2, and CO gases are generated at cell overcharge conditions [72] with EC producing CO_2 and C_2H_4 [117], DEC producing CO and C_2H_6, and DMC producing CO and CH_4 [73]. The dissolution of the generated gases in electrolyte solution, cause a compositional change in the electrolyte which creates a strong concentration gradient in the electrolyte. In addition, certain electrolyte solvent performance indices, such as Li salt diffusion coefficient, Li^+ transference number, and Li salt activity, are affected thereby limiting the transport properties of the electrolyte [73].

5. Formation of SEI layer

The formation of the solid electrolyte interface (SEI) depends largely on the electrode materials, electrolyte salts, and solvents involved [13,53,76–78]. The surface film passivation, which generally follows a classical diffusion-limited process [78], is also influenced by electrolyte additives [2,6,16,80] and the potential window [11]. Most electrolyte solvents of high purity have a decomposition potential of 4.6–4.9 V vs. Li/Li^+, although for lithium ion batteries a potential greater than 5 V is desired [11].

The solvent reduction process generally proceeds either with one-electron [77,81] or two-electron [31,82] transfer between the electrode and the solvent molecules. The salt reduction on the other hand, is initiated by anodic polarization to generate an unstable radical anion [74,78,79,83,84]. The salt anion then undergoes a ring opening decomposition reaction with the solvent to produce inorganic species that precipitates on the surface of the electrode [57,78]. These precipitated inorganic species together with solvated Li^+ are trapped in existing pores on the electrode as the electrode is polarized to potentials below 2.5 V vs. Li/Li^+ [12,13,85,86]. The specific potential is a function of electrode type and solvent [11,87]. The lifetime of the trapped solvated Li^+ within a growing SEI depends on the donor–acceptor properties of the solvent molecules [63]. The binder materials holding the electrode particles together have been reported to react favorably with decomposition species to form species that contribute to the SEI layer [22].

One type of graphite that has been widely used as an anode material is the highly oriented pyrolytic graphite (HOPG). The HOPG has a high degree of preferred crystallographic orientation of the c-axes and remains stable at the temperatures >200 °C. However, due to the anisotropic nature of HOPG, characteristics such as thermal conductivity and electrical resistivity are different in different directions: along the basal plane and along the edge plane. This anisotropic also affects reactive sites, with edge plane having more reactive sites than the basal plane, thus a dense and homogeneous SEI layer is formed on the edge plane that consists of sublayers [27,88] compared to that formed on the edge plane. As illustrated in Fig. 3, the reduction species have "sticky fingers" which improves its adhesion to the graphite particles to improve the robustness of the SEI layer [42,89]. The positively charged alkyl organic moiety aligns with the SEI in such a way that those atoms bearing the partially positive charge serve as the adhesion points and the next layer will attach itself to the SEI layer via coulombic attraction from the negatively charged region on the SEI surface [100].

The SEI thickness is independent of the current density at 20 °C but evolves as the temperature changes [90] thereby aging the SEI film faster [91]. An unfavorable formation temperature (a low of <−30 °C and a high >60 °C) can cause structural changes to the pores structure and create a number of defective sites in the SEI layer [88,92]. This creates species accumulation at these defective sites to increase the amounts of reduction products constituting the SEI layer [1,4]. A low temperature generally affects diffusivity of the limiting reacting species that may result in the formation of a thin and unstable SEI layer [92] and does not affect the irreversible capacity of the batteries at least for first few cycles (<100 cycles) compared to high formation temperature, while a denser SEI would be formed on the edge plane at high temperature for the graphite anode. This thus creates an imbalance in the SEI layer thickness on the HOPG anode electrode. Adding dilithiumphthalocyanine additive significantly controls the imbalances in the SEI layer in thickness on the graphite and enhances Li ions transport rate [102]. The high operating temperature could also initiate the onset of thermal breakdown of the passive film (SEI) in any given type of carbon, which depends on the type of electrolyte salt [75] in the batteries. On the other hand, a moderate (30 °C) temperature will promote the formation of a uniform and less dense SEI layer on the graphite anode, although it may partially dissolve during cell over discharge [22,23].

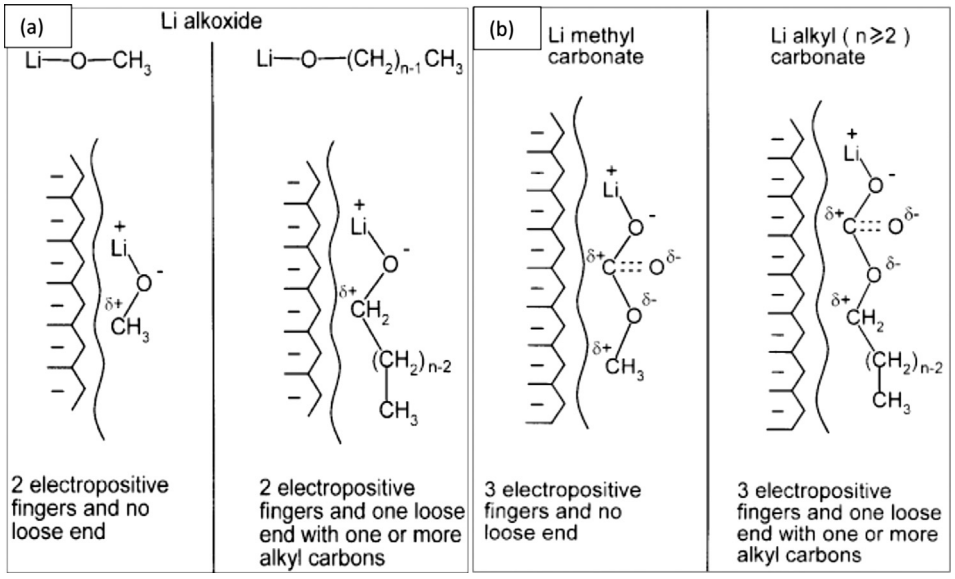

Fig. 3. Schematic of the stick-fingers model of the (a) Li methyl and alkyl carbonate, and (b) methoxide and alkoxide from reduction of the alkyl carbonate on the graphite particles [100] (Reproduced by permission The Electrochemical Society).

5.1. Morphology of the SEI layer

The nature and morphology of the SEI layer on an electrode is a key component of an effective and robust SEI layer. The SEI morphology formed is influenced by the electrode material, electrolytes salts, and solvents involved. For instance, the electrolyte salts $LiClO_4$ and LiTFSI, form porous and spongy SEI morphologies [70,93] with carbonate solvents on a graphite anode. While LiFTSI and LiBOB in a polysiloxane solvent, form a disordered matrix and a gel-like/island film SEI morphologies, respectively (Fig. 4), that accumulate on the HOPG surface [94]. The electrolyte salts: $LiCF_3SO_3$, $LiBF_4$, $LiN(SO_2CF_3)_2$, $LiClO_4$, and LiTFSI are reported to form a leaky SEI layers on the graphite electrode surface in carbonate solvents [24–27], which can be a source of recyclable lithium ions loss [95–97].

The leaky SEI layer can be improved when the lithium ions on the surface react with CO_2, a by-product from EC reduction, to form Li_2CO_3 species on the surface [98]. The Li_2CO_3 species form a layer that bridges the gap that separates Li-rich and Li-deficient islands on the carbon introduced by the leaky SEI layer.

The $LiPF_6$ salt, on the other hand, forms various SEI morphologies depending on the electrolyte solvent and anode electrode materials. It forms porous globules surface film of varied sizes [12,27,28,70] on the graphite electrode with carbonate solvents. These SEI morphologies often function in various ways that prevent lithium ions consumption [99], reduce the electrical path into the graphite particles, and control total interfacial resistance [100,101].

5.2. Factors influencing SEI growth

The SEI growth is generally expected to be fixed by the electrolyte flow rate, electrolyte composition [79], charging current, voltage, temperature, [77,82], and to a lesser degree, the anode to cathode contact pressure [104]. The SEI has been reported to grow linearly with the square root of the time for a range of current densities [105,106]. For the carbonaceous anode, the SEI growth is uniform throughout the graphite electrode even at high C-rate [82,107]. The electrode potential and temperature are other factors that greatly influence the variation in the SEI formation and growth [17,77,97]. A thick SEI layer is formed at a deep discharge state and high formation temperature [67,75,96]. These deep discharge and high formation temperature affect the microstructure of the SEI layer which greatly influences the cell performance [108].

The kinetics of Li^+ transfer at the electrode/electrolyte interface is mostly influenced by the structure and thickness of the SEI layer [35] and the thickness of the growing SEI layer [18,102,103].

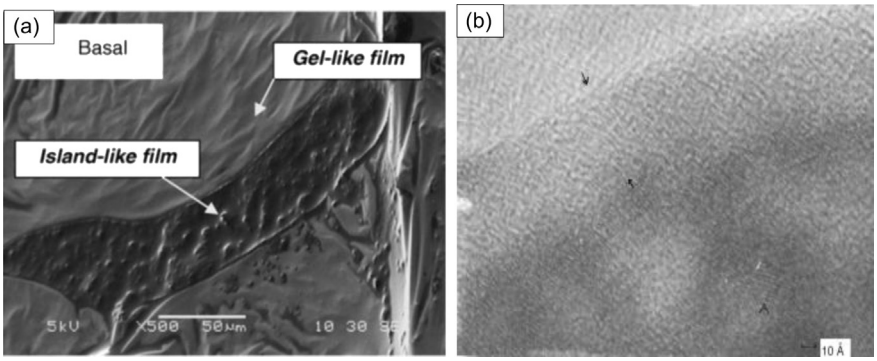

Fig. 4. SEM and TEM micrographs of the SEI layer showing (A) gel/island like [28,110] (Reproduced by permission The Power Sources) and (B) disordered matrix [95] (Reproduced by permission The Electrochemical Society).

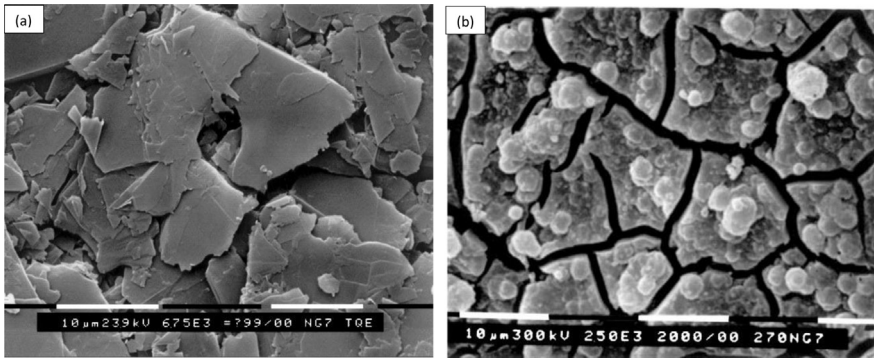

Fig. 5. SEM micrographs showing deposit surface layer resulting from a breakdown of the SEI layer on pristine graphite (a) and cycling condition (b) [90] (Reproduced with permission from Elsevier).

Therefore a thicker SEI creates a high energy barrier for Li^+ insertion/de-insertion at the electrode/electrolyte interface [24] that will increase the Li^+ charge transfer resistance [15].

6. Degradation of the of SEI

An ineffective SEI layer is a source for trapped solvated lithium ions in the growing layer which can lead to the formation of metallic lithium clusters [9,88,95,96]. The trapped solvated Li ions in the growing SEI react with the electrolyte to increase reduction species surface concentration [24] and significantly increases charge transfer resistance [32,109–113]. The accumulated reduction species on the graphite surface decrease the pore size in SEI layer that leads to a sluggish Li^+ intercalation/de-intercalation kinetics.

The reaction of chemical species constituting the SEI layer with H_2O leads to the generation of OPF_2OR, an autocatalytizer, to accelerate the decomposition of the salt that alters SEI layer composition and distorts its structure [79]. This structural change in the SEI layer decreases its ion conductivity at cell storage conditions [82,115] (Fig. 5). At high cell operating temperatures and charge rate, the SEI completely breaks down structurally [90,91] leading to many degradation mechanisms such exfoliation and amorphization occurring at the graphite/electrolyte interface. The interaction of the SEI layer with its surroundings from its formation stage to its eventual degradation is depicted in Fig. 6. The breakdown of the SEI layer results in the percolation of solution inside the bulk graphite electrode, lithium plating and subsequent current collector corrosion [114] and this breakdown temperature of the SEI layer is often a function of the salt reduction reaction temperature [67,92].

On the other hand, a robust and effective SEI layer inhibits further solvent decomposition, prevents solvent co-intercalation, prevents graphite exfoliation and improves cycling efficiency [15–17,85]. In addition, an effective SEI layer will reduce significantly the double layer capacitance [25,108] and increases the ion conductivity [116] in the electrode/electrolyte interface relative to an ineffective SEI layer.

7. Improving SEI layer structure

7.1. Electrolyte additives

7.1.1. Vinylene carbonate (VC) additive

Vinylene carbonate (VC) is extensively used as an additive in many carbonate electrolytes. The VC additive in a carbonate

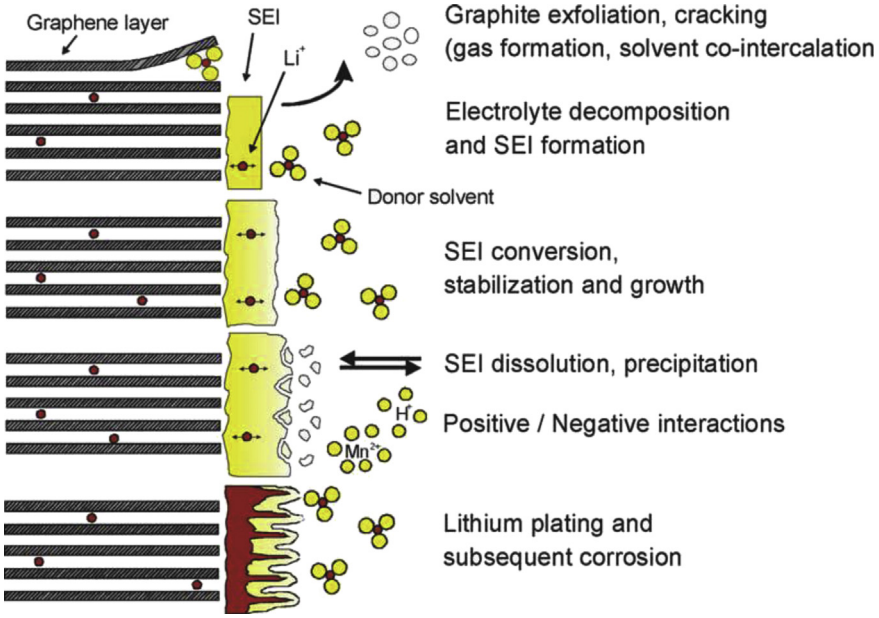

Fig. 6. Schematic diagram showing the SEI interaction with the electrolyte leading to the various interaction [114] (Reproduced with permission from Elsevier).

electrolyte solution undergoes an intermediate reduction reaction to form a stable ion-pair that then undergoes a ring-opening reaction by homolytic C(carbonyl carbon) O-rupture of the carbonate solvent [36,66]. The stable ion-pair is terminated to generate unsaturated complexes of lithium dicarbonates-$(CHOCO_2Li)_2$ and lithium divinylene dicarbonate $(CH{=}CHOCO_2Li)_2$ [116], which are active film-forming products consisting of polymerization products of VC deposited on the electrode [6] and form a SEI layer that enhances lithium ion transport at the electrode/electrolyte interface [34]. The effectiveness of VC as an additive is due to its higher negative reduction potential vs Li^+/Li relative to the supporting solvents such EC, PC DMC, etc so that could reduce well before the supporting solvents and to a lesser extent on its strong solvation. The VC terminating complexes effectively deactivate the reactive sites (radicals and oxides at the defect and edge of the graphite layer) [44,118] and on the cleaved surface of the carbon electrode to prevent the carbonate solvent co-intercalation and direct solvent decomposition on the graphite particle [12].

In addition, the vinylene carbonate additive significantly reduces the amounts of ethylene, propylene, hydrogen and other gases formed at the cathode electrode from decomposition of the carbonate solvent [119]. Other VC based compounds such as 2-cyanofuran (2CF) and ethyl isocyanates [120–122], form good passivation layers on the graphite surface via electropolymerization to protect the graphite from exfoliation in PC based electrolyte solvents.

7.1.2. Other solvent additives

Besides the conventional VC electrolyte additive, other methods have been shown to improve the formation of an effective SEI layer. Some these include the addition of low concentrations of Lewis bases, such as pyridine, hexamethoxy-cyclophosphazene and hexamethylphosphoramide (HMOPA), which prevents the thermal decomposition of dialkyl and cyclic carbonate solvents containing $LiPF_6$ on the surface of Meso Carbon Micro Bead (MCMB) electrodes [37,65]. In a $LiClO_4$/PC electrolyte, where intercalation of lithium ions into MCMB is not possible, the addition of H_2O into the electrolyte [16] facilitates the formation of a LiOH layer that suppresses the PC decomposition and enhances lithium intercalation, while $LiNO_3$ and polysulfide additives form an effective passive film to suppress the further electrolyte decomposition. Inorganic solvent additives of carbon dioxide [2,16,105] react with Li^+ to form a passive film of Li_2CO_3 on graphite intercalation compounds (GICs) to suppress solvent co-intercalation and electrolyte decomposition in PC electrolytes. Sulfur compounds such as ethylene sulfite, sulfur dioxide, and propylene sulfite electrolyte additives have also been employed to improve the properties and qualities of the SEI layer especially in PC-containing electrolytes systems [121,123,124]. These sulfur compounds are reduced at potential 2 V vs. Li^+/Li to form the passivation layers which hinder PC solvent co-intercalation into the graphite layers. The other group of electrolyte additives consists of inorganic compounds of CO_2 N_2O, SO_2 and CS_2 which form good passivation surface species, such as Li_2CO_3, LiO_2, Li_2S and $Li_2S_2O_4$, on the graphite surface to stabilize the SEI layer [125–128].

7.2. Surface modifications

Modification of the surface of the graphite electrode has also been shown to improve SEI structure. Chemical processes, such as attaching long-chain fluoroaliphatic polyxyethylene hydrophobic molecules [108], and formation of self-assemble monolayers, such as $H{-}(CH_2)_{22}{-}(CH_2{-}CH_2{-}O)_{10}{-}H$, to form a dense Li oxide film [115] on the carbon electrode surface have been reported to inhibit electrode passivation and significantly change the double-layer structure and potential distribution. Heat treating the graphite particles, on the other hand, improves the formation of an effective SEI. The heat treated graphite creates a highly crystalline graphite surface with low superficial defects concentrations, low proportion of prism plane surfaces and low impurities levels [129]. This structure ordering increases the amount of active surface sites on the surface and improves the passivation of the SEI layer on the electrode. A combination of high temperature gas treatment and silylation of the graphite surface in aqueous solution has been used to improve SEI effectiveness. In the silylation of the graphite surface, the silane couples with the hydroxyl-containing carbon surface species that facilitates the formation of a passivation film thereby effectively reducing the irreversible charge loss [130] in the electrode.

Another surface modification method is to coat the graphite surface electrode with a thin layer of some active elements such as carbon and copper. These compounds forms a protective coating on the graphite electrode surface [48,131] by covering the catalytic sites on the graphite anode and provides protection towards the formation of surface species, such as LiF, Li_xPF_x and $LiPO_yF_z$ [110] on the carbon surface that also prevent carbon exfoliation especially in PC-based electrolyte. Fig. 7 illustrates a typical surface coating with copper on the graphite particle that significantly improves the surface morphology of the particles to enhance electrochemical reactivity of the particles. Thin surface coating of siloxane has also been used on HOPG electrode, which forms Si–O and C–O-bonds on the graphite surface and silicon/ethylene side chain groups [132] on the electrolyte interface that influences the morphology and electrochemical properties of the passive film and inhibits the formation of gel-like films on the HOPG electrode. The surface

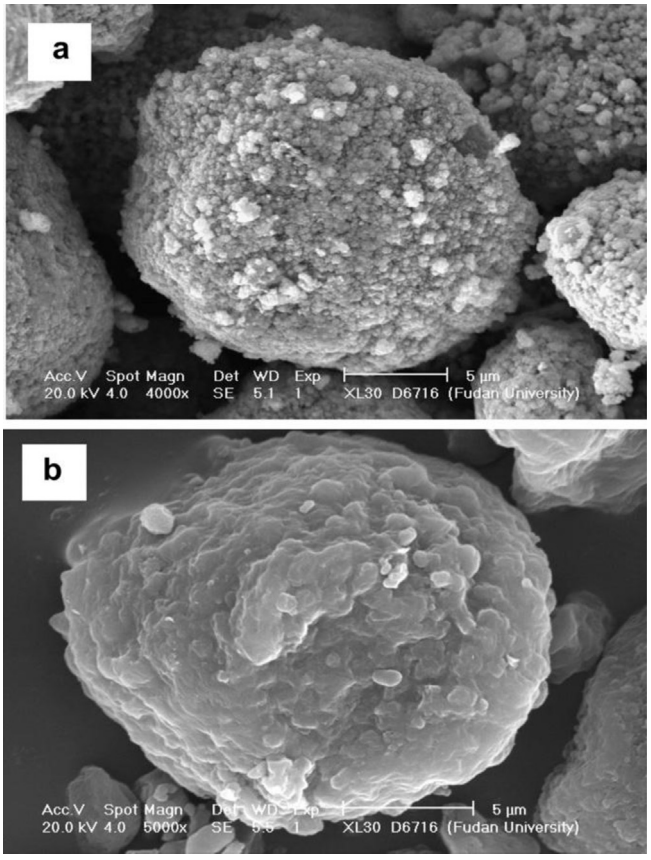

Fig. 7. SEM micrographs of carbon particles (a) coated with copper and (b) the original graphitic carbon particles. [48] (Reproduced with permission from Elsevier).

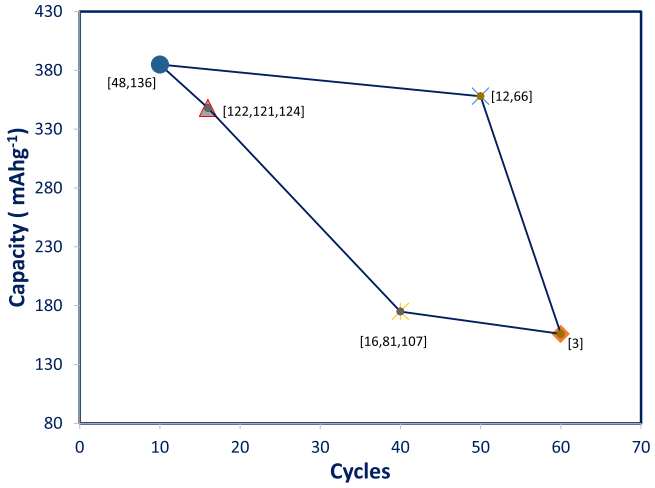

Fig. 8. Extracted plots of capacity improvement of the carbon electrode at different cycles resulting from various surface treatment methods, electrolyte additives, and surface modification on the carbon surface.

modifications on the carbon surface and the various electrolyte additives have been effective in preventing undesirable electrochemical side reactions on the carbon particles surface, and in a bid improves the reversible capacity of the electrode. These capacity improvement of the carbon is shown in Fig. 8 for the first 50 cycles. The different levels capacity improvement results from the type of carbon as well as the electrolyte system employed in batteries.

8. Conclusion

The formation of a stable and effective SEI is critical to attaining high battery cycling efficiency. Widely used carbonaceous anode electrodes generally form a relatively stable SEI layer in most electrolyte salts and carbonates solvents, but this stability can be degraded under certain operable battery conditions. Progress has been made in the development of additives and surface modifications on the carbonaceous anode electrode to sustain a robust SEI layer, but additional improvements and alternative anode materials are still required in order to energy delivery.

References

[1] W.S. Song, G.V. Zhuang, P.N. Ross, J. Electrochem. Soc. 151 (8) (2004) A1162.
[2] A. Wursig, H. Buqa, M. Holzapfel, F. Krumeich, N. Petr, J. Electrochem. Solid-State Lett. 8 (1) (2005) A34.
[3] L. Yang, T. Markmaitree, B.L. Lucht, J. Power Sources 196 (2011) 2251–2254.
[4] B. Fleutot, H. Martinez, B. Pecquenard, J.B. Ledeuil, A. Levasseur, D. Gonbeau, J. Power Sources 180 (2008) 836–844.
[5] J. Shim, R. Kostecki, T. Richardson, X. Song, K.A. Striebel, J. Power Sources 112 (2002) 222–230.
[6] V. Agubra, J. Fergus, Materials 6 (4) (2013) 1310–1325.
[7] N. Kircheva, S. Genies, D. Brun-Buisson, P.X. Thievel, J. Electrochem. Soc. 159 (1) (2012) A18.
[8] B.M. Meyer, N. Leifer, S. Sakamoto, J. Electrochem. Soc. 8 (3) (2005) A145.
[9] G.V. Zhuang, H. Yang, B. Blizanac, P.N. Ross Jr., J. Electrochem. Solid-State Lett. 8 (9) (2005) A411.
[10] M. Herstedt, D.P. Abraham, J.B. Kerr, K. Edstrom, Electrochim. Acta 49 (2004) 5097.
[11] S.B. Lee, S. Pyun, Carbon 40 (2002) 2333–2339.
[12] S.K. Jeong, M. Inaba, R. Mogi, Y. Iriyama, A. Takeshi, Z. Ogumi, Langmuir 17 (2001) 8281–8286.
[13] D. Aurbach, M. Moshkovich, Y. Cohen, A. Schechter, Langmuir 15 (1999) 2947–2960.
[14] C. Huang, S. Zhuang, F. Tu, J. Electrochem. Soc. 160 (2) (2013) A376.
[15] D. Aurbach, E. Yair, C. Chusid, J. Electrochem. Soc. 141 (3) (1994) A603.
[16] K. Kanamura, S. Shiraishi, H. Takezawa, Z. Takehara, Chem. Mater. 9 (1997) 1797–1804.
[17] J.S. Gnanaraj, R.W. Thompson, S.N. Iaconatti, J.F. DiCarlos, J. Electrochem. Solid-State Lett. 8 (2) (2005) A128.
[18] G.V. Zhuang, P.N. Ross, Electrochem. Solid-State Lett. 6 (7) (2003) A136.
[19] D. Aurbach, M. Koltypin, H. Teller, Langmuir 18 (2002) 9000–9009.
[20] K.L. Browning, L. Baggetto, R.R. Unocic, N.J. Dudney, G.M. Veith, J. Power Sources 239 (2013) 341–346.
[21] S. Leroy, F. Blanchard, R. Dedryve're, H. Martinez, B. Carre, D. Lemordant, D. Gonbeau, Surf. Interface Anal. 37 (2005) 773–781.
[22] L.E. Ouatani, R. Dedryvère, J.-B. Ledeuil, C. Siret, P. Biensan, J. Desbrières, D. Gonbeau, J. Power Sources 189 (2009) 72–80.
[23] D. Lu, M. Xu, L. Zhou, A. Garsuch, B. Lucht, J. Electrochem. Soc. 160 (5) (2013) A3138.
[24] H. Ota, Y. Sakata, J. Sasahara, E. Yasuwa, J. Electrochem. Soc. 151 (3) (2004) A437.
[25] C. Fringant, A. Tranchant, R. Messina, Electrochim. Acta 40 (4) (1995) 513–523.
[26] A. Kominato, E. Yasukawa, N. Sato, T. Ijuuin, H. Asahina, S. Mori, J. Power Sources 68 (1997) 471–475.
[27] S. Shiraishi, K. Kanamura, Z. Takehara, Langmuir 13 (1997) 3542–3549.
[28] T. Li, L. Xing, W. Li, Y. Wang, M. Xu, F. Gu, S. Hu, J. Power Sources 244 (2013) 668–674.
[29] Y. Wang, S. Nakamura, M. Ue, P.B. Balbuena, J. Am. Chem. Soc. 123 (2001) 11708–11718.
[30] Y. Okamoto, J. Electrochem. Soc. 160 (2) (2013) A404.
[31] R. Dedryvère, H. Martinez, S. Leroy, D. Lemordant, F. Bonhomme, P. Biensan, D. Gonbeau, J. Power Sources 174 (2007) 462–468.
[32] D. Aurbach, M. Mashkovich, J. Electrochem. Soc. 145 (8) (1998) A2629.
[33] P. Novak, M. Lanz, D. Allia, B. Rykart, J. Paniz, O. Haas, J. Power Sources 97 (2001) 39–46.
[34] F. Joho, P. Novák, Electrochim. Acta 45 (2000) 3589–3599.
[35] Y. Yamada, Y. Iriyama, T. Abe, Z. Ogumi, Langmuir 25 (21) (2009) 12766–12770.
[36] C.L. Campion, W. Li, W.B. Euler, B.L. Lucht, B. Ravdel, J.F. DiCarlo, R. Gitzendanner, K.M. Abraham, J. Electrochem. Solid-State Lett. 7 (7) (2004) A194.
[37] S. Leroy, Hartinez, R. Dedryvere, D. Lemordant, D. Goneau, Appl. Surf. Sci. 253 (2007) 4895–4905.
[38] A. Schechter, D. Aurbach, Langmuir 15 (1999) 3334–3342.
[39] M. Broussely, P.H. Biensan, F. Bonhomme, P.H. Balnchard, S. Herreyre, K. Nechev, R.J. Staniewicz, J. Power Sources 146 (2005) 90–96.
[40] H. Yamada, Y. Watanabe, I. Moriguchi, T. Kudo, Solid State Ionics 179 (2008) 1706–1709.
[41] M. Wolfgang, C. Lu, P. Novak, J. Electrochem. Soc. 158 (2011) A1478.
[42] H. Wang, Y. Jang, B. Huang, R.D. Sadoway, Y.M. Chiang, J. Electrochem. Soc. 146 (1999) A473.
[43] D. Aurbach, M.D. Levi, E. Levi, A. Schechter, J. Phys. Chem. B 101 (1997) 2195–2206.
[44] Y. Wang, P.B. Balbuena, J. Phys. Chem. B 106 (2002) 4486–4495.
[45] M. Matsui, K. Dokko, K. Kanamura, J. Power Sources 177 (2008) 184–193.
[46] E. Yair, J. Electrochem. Solid-State Lett. 2 (5) (1999) A212.
[47] Y. Geronov, F. Schwager, R.H. Muller, J. Electrochem. Soc. 129 (7) (1982) A1422.
[48] J. Gao, L.J. Fu, H.P. Zhang, T. Zhang, Y.P. Wu, H.Q. Wu, J. Electrochem. Commun. 8 (2006) 1726–1730.
[49] M. Wolfgang, N. Tran, G. Dietrich, M.E. Spahr, N. Petr, Carbon 47 (2009) 2727–2732.
[50] S.S. Zhang, K. Xu, T.R. Jow, J. Electrochem. Solid-State Lett. 5 (9) (2002) A206.
[51] H. Nakamura, H. Komatsu, M. Yoshio, J. Power Sources 62 (1996) 219–222.
[52] Z. Lu, Y. Li, Y. Guo, J. Power Sources 156 (2006) 555–559.
[53] E. Endo, K. Tanaka, K. Sekai, J. Electrochem. Soc. 147 (11) (2000) A4029.
[54] S. Wilken, P. Johansson, P. Jacobsson, Solid State Ionics 225 (2012) 608–610.
[55] C.L. Campion, W. Li, B.L. Lucht, J. Electrochem. Soc. 152 (12) (2005) A2327.
[56] S.E. Sloop, J.B. Kerr, K. Kinoshita, J. Power Sources 119 (2003) 330–337.
[57] B. Ravdel, K.M. Abraham, R. Gitzendanner, J. DiCarlo, B. Lucht, C. Campion, J. Power Sources 119 (2003) 805–810.
[58] S.W. Song, S.W. Baek, Electrochim. Acta 54 (2009) 1312–1318.
[59] K. Tasaki, K. Kand, S. Nakamura, M. Ue, J. Electrochem. Soc. 150 (12) (2003) A1628.
[60] L. Terborg, S. Weber, F. Blaske, S. Passerini, M. Winter, K. Uwe, S. Nowak, J. Power Sources 242 (2013) 832–837.
[61] T. Kawamura, S. Okadaa, J. Yamaki, J. Power Sources 156 (2006) 547–554.
[62] Y.G. Ryu, S. Pyun, J. Electroanal. Chem. 433 (1997) 97–105.
[63] D. Rahner, J. Power Sources 81 (1999) 358–361.
[64] K. Kumai, T. Ikeya, K. Ishihara, T. Iwahori, N. Imanishi, Y. Takeda, O. Yamamoto, J. Power Sources 70 (1998) 235–239.
[65] S.E. Sloop, J.K. Pugh, S. Wang, J.B. Kerr, K. Kinoshita, J. Electrochem. Solid-State Lett. 4 (4) (2001) A42.
[66] W. Li, C. Campion, B.L. Lucht, B. Ravdel, J. Dicarlo, K.M. Abraham, J. Electrochem. Soc. 152 (7) (2005) A1361.
[67] H. Maleki, G. Deng, A. Anani, J. Howard, J. Electrochem. Soc. 146 (9) (1999) A3224.
[68] P. Röder, N. Baba, K.A. Friedrich, H.-D. Wiemhöfer, J. Power Sources 236 (2013) 151–157.
[69] K. Edstrom, A.M. Anderson, A. Bishop, L. Framsson, J. Lingren, Ahussenius, J. Power Sources 97 (2001) 87–91.
[70] T. Yu, Y. Orikasa, M. Mogi, M. Oishi, J. Power Sources 196 (2011) 10679–10685.

[71] S. Mori, H. Asahina, H. Suzuki, A. Yonei, K. Yokoto, J. Power Sources 68 (1997) 59–64.
[72] N. Dupré, J.F. Martin, J. Oliveri, P. Soudana, A. Yamada, R. Kanno, D. Guyomard, J. Power Sources 196 (2011) 4791–4800.
[73] A.M. Haregewoin, E.G. Leggesse, J. Chiang, F.M. Wang, B. Hwang, S.D. Lin, J. Power Sources 244 (2013) 318–327.
[74] K. Kumai, H. Miyashiro, Y. Kobayashi, K. Takei, R. Ishikawa, J. Power Sources 81 (1999) 715–719.
[75] C.R. Yang, Y.Y. Wang, C.C. Wan, J. Power Sources 72 (1998) 66–70.
[76] D. Peramunage, K.M. Abraham, J. Electrochem. Soc. 145 (8) (1998) A2615.
[77] X. Wu, H. Li, L. Chen, X. Huang, Solid State Ionics 149 (2002) 185–192.
[78] G.V. Zhuang, P.N. Ross, H. Yang, K. Xu, T.R. Jow, J. Electrochem. Solid-State Lett. 9 (2) (2006) A64.
[79] E.L. Littauer, K.C. Tsai, J. Electrochem. Soc. 123 (7) (1976) A964.
[80] J.S. Bridel, S. Grugeon, S. Laruelle, J. Hassoun, P. Reale, B. Scrosati, J.M. Tarascon, J. Power Sources 195 (2010) 2036–2043.
[81] J. Li, H. Li, Z. Wang, L. Chen, X. Huang, J. Power Sources 107 (2002) 1–4.
[82] K. Takei, K. Kumai, Y. Kobayashi, H. Miyashiro, T. Iwahori, T. Uwai, H. Ue, J. Power Sources 54 (1995) 171–174.
[83] M. Holzapfel, F. Alloin, R. Yazami, Electrochim. Acta 49 (2004) 581–589.
[84] J.O. Besenhard, M. Winter, J. Yang, W. Biberacher, J. Power Sources 54 (1995) 228–231.
[85] M.R. Wagner, P.R. Raimann, A. Trifonova, K.-C. Moeller, J.O. Besenhard, M. Winter, Electrochem. Solid-State Lett. 7 (7) (2004) A201.
[86] S.K. Jeong, M. Inaba, Y. Iriyama, T. Abe, Z. Ogumi, J. Power Sources 119 (2003) 555–560.
[87] G.V. Zhuang, K. Xu, T.R. Jow, P.N. Ross, J. Electrochem. Solid-State Lett. 7 (8) (2004) A224.
[88] Y. Domi, M. Ochida, S. Tsubouchi, H. Nakagawa, T. Yamanaka, T. Doi, T. Abe, Z. Ogumi, J. Phys. Chem. C 115 (2011) 25484–25489.
[89] E. Yair, Electrochem. Solid-State Lett. 2 (5) (1999) 212–214.
[90] D. Zane, A. Antonini, M. Pasquali, J. Power Sources 97 (2001) 146–150.
[91] A.Z. Shekhtman, J. Power Sources 54 (1995) 433–434.
[92] A.M. Andersson, M. Herstedt, A.G. Bishop, K. Edstrom, Electrochim. Acta 47 (2002) 1885–1898.
[93] A. Naji, J. Ghanbaj, P. Willmann, B. Humbert, D. Billaud, J. Power Sources 62 (1996) 141–143.
[94] H. Nakahara, S. Nutt, J. Power Sources 158 (2006) 1386–1393.
[95] J.S. Gnanaraj, R.W. Thompson, S.N. Iaconatti, J.F. DiCarlo, K.M. Abraham, J. Electrochem. Solid-State Lett. 8 (2) (2005) A128.
[96] M. Safaria, C. Delacourt, J. Electrochem. Soc. 158 (10) (2011) A1123.
[97] M. Kassem, C. Delacourt, J. Power Sources 235 (2013) 159–171.
[98] E. Yair, D. Aurbach, J. Power Sources 54 (1995) 281–288.
[99] N. Choi, K.H. Yew, H. Kim, S.S. Kim, W. Choi, J. Power Sources 172 (2007) 404–409.
[100] H. Li, X. Huang, L. Chen, J. Electrochem. Solid-State Lett. 1 (6) (1998) 241.
[101] C.R. Yang, J.Y. Song, Y.Y. Wang, C.C. Wan, J. Appl. Electrochem. 30 (2000) 29–34.
[102] D. Rahner, S. Machill, K. Siury, J. Power Sources 68 (1997) 69–74.
[103] N. Munichandraiah, L.G. Scanlon, R.A. Marsh, J. Power Sources 72 (1998) 203–210.
[104] M. Dolle, S. Grugeon, B. Beaudion, L. Dupont, J.-M. Tarascon, J. Power Sources 97 (2001) 104–106.
[105] C.A. Caldas, M.C. Lopes, I.A. Carlos, J. Power Sources 74 (1998) 108–112.
[106] M. Ota, S. Izuo, K. Nishikawa, Y. Fukunak, E. Kusaka, R. Ishii, J.R. Selman, J. Electroanal. Chem. 559 (2003) 175–183.
[107] M.B. Pinson, M.Z. Bazant, J. Electrochem. Soc. 160 (2) (2013) A243.
[108] M. Lu, H. Cheng, Y. Yang, Electrochim. Acta 53 (2008) 3539–3546.
[109] C. Tran, J. Kafle, X.Q. Yang, D. Qu, Carbon 49 (2011) 1266–1271.
[110] H. Nakahara, S.Y. Yoon, T. Piao, F. Mansfeld, S. Nutt, J. Power Sources 158 (2006) 591–599.
[111] N. Dupré, J.F. Martin, J. Degryse, V. Fernandez, P. Soudan, D. Guyomard, J. Power Sources 195 (2010) 7415–7425.
[112] S. Xiaong, K. Xie, Y. Diao, X. Hong, J. Power Sources 246 (2014) 840–845.
[113] D.P. Abraham, M.M. Furczon, S.-H. Kang, D.W. Dees, A.N. Jansen, J. Power Sources 180 (2008) 612–620.
[114] J. Vetter, P. Novak, M.R. Wagner, C. Veit, K.C. Moller, J.O. Besenhard, M. Winter, M. Wohlfahrt-Mehrens, C. Vogler, A. Hammouche, J. Power Sources 147 (2005) 269–281.
[115] M.L. Granvalet-Mancini, T. Hanrath, D. Teeters, Solid State Ionics 135 (2000) 283–290.
[116] R.N. Mason, M. Smith, T. Andrews, D. Teeters, Solid State Ionics 118 (1999) 129–133.
[117] Y. Wang, S. Nakamura, K. Tasaki, P.B. Balbuena, J. Am. Chem. Soc. 124 (2002) 4408–4421.
[118] O. Matsuoka, A. Hiwara, T. Omi, M. Toriida, T. Hayashi, C. Tanaka, Y. Saito, T. Ishida, H. Tan, S.S. Ono, S. Yamamoto, J. Power Sources 108 (2002) 128–138.
[119] H. Buqa, A. Würsig, J. Vetter, M.E. Spahr, F. Krumeich, P. Novák, J. Power Sources 153 (2006) 385–390.
[120] C. Korepp, H.J. Santner, T. Fujii, M. Ue, J.O. Besenhard, K.-C. Moller, M. Winter, J. Power Sources 158 (2006) 578–582.
[121] G.H. Wrodnigg, J.O. Besenhard, M. Winter, J. Electrochem. Soc. 146 (1999) A470.
[122] C. Korepp, W. Kern, E.A. Lanzer, P.R. Raimann, J.O. Besenhard, M.H. Yang, K.-C. Moller, D.-T. Shieh, M. Winter, J. Power Sources 174 (2007) 387–393.
[123] V. Ein-Eli, S.R. Thomas, V.R. Koch, J. Electrochem. Soc. 143 (1996) L195.
[124] M.W. Wagner, C. Liebenow, J.O. Besenhard, J. Power Sources 68 (1997) 328–332.
[125] X. Bourrat, Carbon 31 (1993) 287.
[126] J.N. Reimers, E.W. Fuller, E. Rossen, J.R. Dahn, J. Electrochem. Soc. 140 (1993) A3396.
[127] S. Kuroda, N. Tobori, M. Sakuraba, Y. Sato, J. Power Sources 924 (2003) 119–121.
[128] E. Grivei, J.B. Soupart, H. Smet, H. Lahdily, ITE Battery Lett. 1 (1999) 64.
[129] M.E. Spahr, H. Buqa, A. Würsig, D. Goers, L. Hardwick, N. Petr, F. Krumeich, J. Dentzer, C. Vix-Guter, J. Power Sources 153 (2006) 300–311.
[130] H. Buqa, C.H. Grogger, M.V.S. Alvavarez, J.O. Besenhard, M. Winter, J. Power Sources 97 (2001) 126–128.
[131] H. Nakahara, S.Y. Yoon, S. Nutt, J. Power Sources 160 (2006) 548–557.
[132] J.S. Sakamoto, F. Wudl, B. Dunn, Solid State Ionics 144 (2001) 295–299.